Polymer 51 (2010) 5100–5106

Contents lists available at ScienceDirect

Polymer

journal homepage: www.elsevier.com/locate/polymer

A novel shape memory polynorbornene functionalized with poly(ε-caprolactone) side chain and cyano group through ring-opening metathesis polymerization

Dan Yang [a], Wei Huang [a], Jiahui Yu [b,*], Jisen Jiang [c], Liya Zhang [a], Meiran Xie [a,*]

[a] Department of Chemistry, East China Normal University, Shanghai 200062, PR China
[b] Institute for Advanced Interdisciplinary Research, East China Normal University, Shanghai 200062, PR China
[c] Department of Physics, Center of Functional Nanomaterials and Devices, East China Normal University, Shanghai 200241, PR China

ARTICLE INFO

Article history:
Received 18 June 2010
Received in revised form
29 August 2010
Accepted 3 September 2010
Available online 15 September 2010

Keywords:
Polynorbornene
Ring-opening metathesis polymerization (ROMP)
Shape memory polymer (SMP)

ABSTRACT

A novel functionalized norbornene-based copolymer with long poly(ε-caprolactone) side chain and cyano group was synthesized in the combination of ring-opening polymerization and ring-opening metathesis polymerization, which was characterized by means of ^{1}H NMR, gel permeation chromatography, thermogravimetry, differential scanning calorimetry, wide-angle X-ray diffraction, and stress–strain measurements. The shape memory effect of the copolymer was evaluated by dynamical mechanical analysis, shape recovery ability, and shape recovery speed. Having the properties of the good shape fixity and the large shape recovery, the functionalized polynorbornene copolymer is expected to use as a potential shape memory material.

1. Introduction

Shape memory materials are the compounds that could vary the shapes according to the external stimulus such as temperature, light, and pH [1]. Decades of intensive studies have contributed to the discovery of several shape memory systems such as shape memory alloy [2–4], shape memory ceramic [5,6] and shape memory polymer (SMP) [7–19], among which the SMP with large recoverable deformation and low recovery temperature is received increasing attention. Since the first SMP methacrylic acid ester was synthesized and used as a denture material, the SMPs are fairly developed and find their way in broad applications including sensors, self-repairing bodies, actuators, and medical implants [4,18,20,21]. Accordingly, excellent shape memory effects have been observed with polyurethane, polynorbornene, styrene-butadiene copolymers, cross-linked polyethylene, epoxy-based polymers and others [8,22–26]. Basically, the SMPs comprise at least two phases, the reversible phase and the frozen phase. The frozen phase associated with the higher transition temperature (T_{trans}) of a crystallization temperature (T_c) or a glass transition temperature (T_g) works as a physical cross-linker of the polymer chains, which is contributed to the permanent shape, while the reversible phase with the lower T_{trans} of T_c or T_g plays the role of a molecular switch. SMPs go through two phases above and below this "transition temperature" repeatedly. Meanwhile, the mechanical energy exerted on the material during deformation is stored. When required, the polymer will recover its permanent shape through the restoration of network chain conformational entropy.

Poly(ε-caprolactone) (PCL) is not only known as biodegradable polymer in the extensive biomedical applications [22], but also a better choice in preparing SMPs as switching segments since the temperature of melting point is around 60 °C and it can be decreased by reducing the molecular weight [27]. At present, the major synthetic method of the polymer is ring-opening polymerization (ROP), which gives tailored molecular weights of PCL by adjusting monomer feed ratios. However, as materials PCL was tarnished by its low modulus and high crystallinity. Therefore, it is usually used in the copolymers like shape memory polyurethanes [7] with the aim of improving mechanical properties and crystallization behavior. In order to obtain uniform structure of the copolymer, the ring-opening metathesis polymerization (ROMP) is invited, since ROMP is considered as a powerful and promising synthetic tool with the capability of the control over the polymer molecular weight and structure. Especially, ROMP excels in preparing polyolefins like polynorbornene (PNBE) from the strained cyclic olefins giving stereoregular and monodisperse polymers and copolymers [28]. With the advancement in second-generation ruthenium metathesis initiator that containing *N*-heterocyclic carbene as co-ligand, the

* Corresponding authors. Tel.: +86 21 62233493; fax: +86 21 62232414.
E-mail addresses: jhyu@sist.ecnu.edu.cn (J. Yu), mrxie@chem.ecnu.edu.cn (M. Xie).

0032-3861/$ – see front matter © 2010 Elsevier Ltd. All rights reserved.
doi:10.1016/j.polymer.2010.09.009

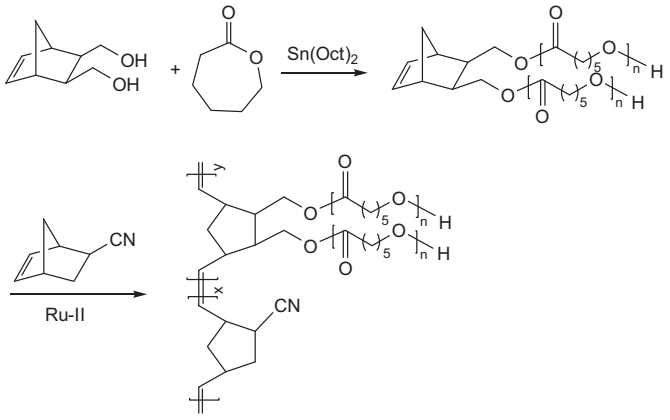

Scheme 1. Synthesis of polynorbornene with PCL side chain and cyano group.

activity of ruthenium-based system in ROMP has raised tremendously with more functional group tolerance such as polar cyano group. There are a few reports on ROMP exploring the scope of ruthenium initiators in norbornene derivatives bearing cyano groups [29,30]. It is well known that norbornene-based polymers are a kind of amorphous polymer with high thermal stability, optical transparency, low dielectric constant, and shape memory abilities in broad applications. However, as used in shape memory materials, PNBE is required high molecular weight to attain a certain mechanical strength that brings about issues in processing.

Based on the consideration above we design a shape memorable copolymer with PCL side chains and cyano functional groups attached to PNBE backbones in the combination of ROP and ROMP as shown in Scheme 1. On the one hand, it forms the microphase segregation structure which is essential for the shape memory effect and improves the mechanical strength of PNBE for choosing the crystalline PCL as side chains to amorphous PNBE backbones. On the other hand, the copolymerization with norbornene derivatives could improve the brittle and poor processible properties of PNBE and the incorporation of functional cyano group in the polymer could dramatically enhance the strength of the materials since cynao group with strong polarity makes the polymer chain more liable to aggregate. Therefore, we prepared polynorbornene functionalized with PCL side chains and cyano group through ROMP. The material molded from the copolymer possesses the typical characteristics of both shape memory effect and thermoplasticity. As a result, this kind of material offers an opportunity for manufacturing through the thermoplastic molding that can be remelted and cooled time after time without undergoing any appreciable chemical change and recycling into a various uses. We provide an appraisal of the thermal, mechanical, and the shape recovery characteristics of the copolymers.

2. Experimental

2.1. Materials

[1,3-Bis-(2,4,6-trimethylphenyl)-2-imidazolidinylidene)dichloro-(phenylmethylene)-(tricyclohexylphosphine)ruthenium] (second generation Grubbs catalyst, Ru-II), 5-norbornene-exo,exo-2,3-dicarboxylicanhydride (>98%), lithium aluminum hydride (95%), tin(II) 2-ethylhexanoate ($Sn(Oct)_2$, 95%), acrylonitrile, dicyclopentadiene, and ε-caprolactone (CL, 99%) were purchased from Aldrich or Alfa Aesar and used without purification. Solvents were distilled over drying agents under nitrogen prior to use; dimethyl sulfoxide (DMSO), chloroform ($CHCl_3$) from calcium hydride; tetrahydrofuran (THF) from sodium/benzophenone. 5-Cyano bicylco[2.2.1]hept-2-ene and exo,exo-bicyclo[2.2.1]hept-5-ene-2,3-dimethanol were synthesized according to the literature procedures [31,32].

Polymerizations were carried out in Schlenk tubes under dry nitrogen atmosphere.

2.2. Characterization

^{1}H NMR (500 MHz) spectra were recorded using tetramethylsilane as an internal standard in DMSO-d_6 and $CDCl_3$ on a Bruker DPX spectrometer. Elemental analysis was carried out with an ELEMENTAR Vario EL3. Gel permeation chromatography (GPC) was used to calculate relative molecular weights and molecular weight distributions equipped with a Waters 1515 Isocratic HPLC pump, a Waters 2414 refractive index detector, and a set of Waters Styragel columns (7.8 × 300 mm, 5 μm bead size; 10^3, 10^4, and 10^5 Å pore size). GPC measurements were carried out at 35 °C using THF as the eluent with a flow rate of 1.0 mL min^{-1}. Differential scanning calorimetry (DSC) was carried out using TA Instruments Q2000 equipped with a refrigerated cooling accessory and an empty aluminum pan as a reference, samples (amount 10 mg) were examined in aluminum pans under an atmosphere of dry nitrogen, the temperature range was from −80 °C to 240 °C, and the measurements were performed at a heating or cooling rate of 10 °C min^{-1}. Thermal gravimetric analysis (TGA) was performed using a SDTA851e/SF/1100 TGA Instrument under N_2 flow at a heating rate of 10 °C min^{-1} from 0 to 800 °C. X-ray diffraction (XRD) analyses were carried out on a Bruker D8 Advance, X-ray diffractometer with Cu-K_α radiation at a wavelength of 1.54 Å. The 2θ angle ranged from 3° to 40°, and the step size and scan rate were 0.02° and 2° min^{-1}, respectively. Tensile test was carried out by a universal testing machine (Instron RG 3010 made in China) using a dumbbell type specimens at room temperature. The gauge length was 20 mm and crosshead speed was 10 mm min^{-1} · 10 g of Copolymer was dissolved in 120 mL of $CHCl_3$ at 50 °C, concentrated to about 30 mL, and the solution was cast onto a glass plate keeping for 6 h and then vacuumizing for 48 h at room temperature to remove $CHCl_3$. Finally, die-cut dumbbell type specimens [50.0 mm (length) × 3.1 mm (width) × 1.5 mm (thickness)]. Dynamic mechanical analysis (DMA) was determined with a dynamic mechanical thermal analyzer (Perkin Elmer Q800), using a tension mode at a heating rate of 3 °C min^{-1} and 1 Hz. The sample was the solution cast film [16.91 mm (length) × 5.50 mm (width) × 1.55 mm (thickness)].

2.3. Preparation of macromonomer norbornene-graft-poly (ε-caprolactone)(NBE-g-PCL)

Macromonomers were synthesized via ROP of CL using exo,exo-bicyclo[2.2.1]hept-5-ene-2,3-dimethanol as the initiator and Sn

Table 1
Characteristics of macromonomers by ring-opening polymerization.

Macromonomer	[CL]:[OH]:[$Sn(Oct)_2$]	Conversion (%)[a]	$M_{n,GPC}$[b] (×10^3, g/mol)	M_w/M_n[b]	$M_{n,NMR}$[c] (×10^3, g/mol)
NBE-g-PCL_{38}	4800:80:1	80	5.0	1.2	4.5
NBE-g-PCL_{76}	1500:25:1	86	9.4	1.4	8.8

Reaction conditions: polymerization temperature = 110 °C, polymerization time = 48 h.
[a] Obtained gravimetrically from the dried polymer.
[b] Measured by GPC analysis in THF.
[c] $M_{n,NMR} = (S_f/2S_{a'}) \times M_{CL} + M_{initiator}$ was obtained by ^{1}H NMR spectroscopy, where $M_{CL} = 114$ and $M_{initiator} = 154$ are the molar masses of CL and initiator, respectively.

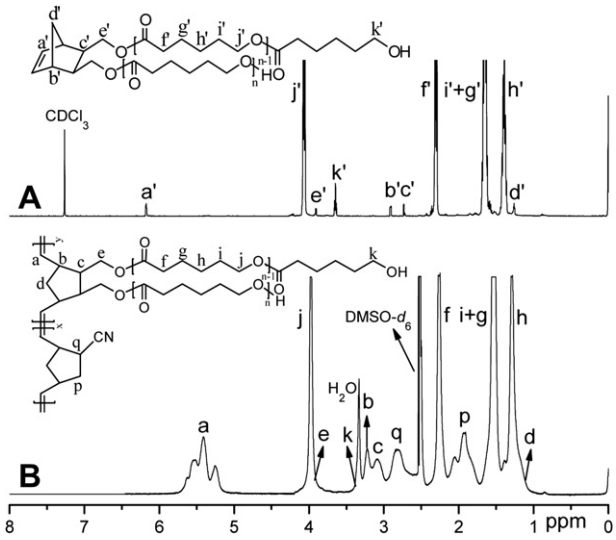

Fig. 1. ^{1}H NMR spectra for (A) macromonomer NBE-*g*-PCL$_{38}$ and (B) copolymer **1**.

$(Oct)_2$ as the catalyst. Typically, the initiator (0.8 g, 5.0 mmol) and CL (34.2 g, 300 mmol) were charged to a Schlenk flask with a magnetic stirring bar, and a solution of $Sn(Oct)_2$ (25.3 mg, 62.5 μmol) in 1 mL of toluene was added using a syringe. The reaction mixture was degassed via three freeze-pump-thaw cycles and then immersed in a thermostated oil bath at 110 °C for 48 h. The crude product was dissolved in THF, and the solution was dropped into an excessive amount of methanol to afford the precipitates. This procedure was repeated three times to obtain white solids. The product was dried in a vacuum oven until a constant weight was obtained. ^{1}H NMR ($CDCl_3$): δ (ppm) 6.17 (s, 2H, olefinic protons on the norbornene ring), 4.07–4.05 (m, CH_2OCO on PCL), 3.91 (m, CH_2OCO-PCL), 3.66–3.63 (t, PCL-CH_2OH), 2.92 (m, 2H, 2× CH on the norbornene ring), 2.74 (m, 2H, 2× CH on the norbornene ring), 2.31–2.28 (m, $OCOCH_2$ on PCL), 1.67–1.63 (m, CH_2 on PCL) 1.40–1.37 (m, CH_2 on PCL), 1.31 (s, 2H, CH_2 on the norbornene ring). GPC: $M_n = 5000$, $M_w/M_n = 1.2$; NMR: $M_n = 4500$.

2.4. General ring-opening metathesis polymerization procedures for the syntheses of copolymers polynorbornene-graft-poly(ε-caprolactone)(PNBE-g-PCL)

In a nitrogen-filled Schlenk tube, a solution of Ru-II (98 mg, 120 μmol) in 20 mL of degassed $CHCl_3$ was added to a solution of NBE-*g*-PCL ($M_{n,NMR} = 4500$; 13.5 g, 3.0 mmol) and 5-cyano bicylco[2.2.1]hept-2-ene (7.14 g, 60.0 mmol) in 280 mL of $CHCl_3$, which were degassed with three freeze-vacuum-thaw cycles, to give a macromonomer concentration of 0.01 mol L^{-1}. The pink solution was stirred at 70 °C under N_2 for 12 h. The color of the solution changed from pink to light yellow. The polymerization was terminated by the addition of 500 equiv. of ethyl vinyl ether and stirred for an additional 30 min. The reaction mixture was then poured into excess cold methanol with stirring, and the precipitates were purified by Soxhlet extractor using acetone as solvent to remove the unreacted macromonomer, resulting in a white solid. ^{1}H NMR (DMSO-d_6): δ (ppm) 5.55–5.26 (m, olefinic protons on the backbone), 3.98 (s, CH_2OCO on PCL), 3.88, (m, CH_2OCO-PCL), 3.4 (t, PCL-CH_2OH), 3.23–3.16 (m, 2H, 2× CH on the norbornene ring), 3.14–3.05 (m, 2H, 2× CH on the norbornene ring), 2.92–2.66 (m, CH–CN), 2.26 (s, $OCOCH_2$ on PCL), 2.06–1.93 (m, CH_2 on the norbornene units), 1.54 (s, CH_2 on PCL), 1.42 (s, 2H, CH_2 on the norbornene ring), 1.29 (s, CH_2 on PCL). GPC: $M_n = 72000$, $M_w/M_n = 1.78$; Elem. Anal. Calcd.: C, 71.90; H, 8.13; N, 5.88. Found: C, 71.17; H, 8.19; N, 5.67.

3. Results and discussion

3.1. Syntheses of macromonomers

Scheme 1 shows the general reaction pathway used for the synthesis of the norbornene-based macromonomer with two PCL side chains. The exo,exo-bicyclo[2.2.1]hept-5-ene-2,3-dimethanol was prepared for initiating ROP of CL. ROP is considered as a successful procedure for controlling the synthesis of aliphatic polyesters such as polylactide, polyglycolide, polymandelide, polyvalerolactone, or PCL [33] and the $Sn(Oct)_2$ is chosen as the catalyst for its efficiency and extensive use in the ROP of various lactones and lactides [34]. The polymerization is conducted at 110 °C for 24 h. The conversion and the molecular weight increase by enlarging the molar ratio of $Sn(Oct)_2$ to CL. The molecular characteristics of macromonomers are shown in Table 1. All these samples have been characterized by ^{1}H NMR and GPC. The molecular weights (M_n) are 5000 and 9400 with monomodal GPC trace and the molecular weight distributions (M_w/M_n) are 1.2 and 1.4 under two different feed ratios.

In order to confirm the structure of the macromonomers, ^{1}H NMR spectrum is measured and shown in Fig. 1A. The chemical shift corresponding to olefinic signals on the norbornene ring (6.17 ppm) testifies the attachment of the norbornyl group. The signal related to methylene protons of $-CH_2OH$ (3.71 ppm) disappears after ROP of CL initiated by alcohol and a new signal at 3.66–3.63 ppm for protons of $-CH_2CH_2OH$ on PCL chain is observed, which means the side chains of PCL are virtually formed. By comparing the peak integration area (S) of methylene protons of $OCOCH_2$ (H_f, 4 protons) from PCL at 2.31–2.28 ppm with that of olefinic protons of CH=CH ($H_{a'}$, 2 protons) from norbornyl group at 6.17 ppm, it is possible to determine PCL-to-norbornene molar ratio from the integral ratio $n = (S_f/4H):(S_{a'}/2H) = (S_f/2S_{a'})$ for calculating the average number of CL units in PCL chain end-capped with norbornene group. Through ^{1}H NMR analysis [35], we confirm that the macromonomer NBE-*g*-PCL$_{38}$ contains 38 CL units ($n = 38$) with a number average molecular weight of 4500 and the macromonomer NBE-*g*-PCL$_{76}$ contains 76 CL units ($n = 76$) with a number average molecular weight of 8800.

Table 2
Characteristics of copolymers by ring-opening metathesis polymerization.

Copolymer	M_1	$[M_1]:[M_2]:[Cat]$[a]	t (h)	Yield (%)[b]	$M_{n,GPC}$ (×10^3, g/mol)[c]	M_w/M_n[c]
1	NBE-*g*-PCL$_{38}$	25:500:1	12	50	72.0	1.78
2	NBE-*g*-PCL$_{76}$	25:1000:1	24	54	151.0	1.60
3	NBE-*g*-PCL$_{76}$	25:500:1	24	49	131.0	1.55

Reaction conditions: $[Macromonomer]_0 = 0.01$ mol L^{-1}, polymerization temperature = 70 °C.
[a] Molar ratios of macromonomer (M_1) to 5-cyano bicyclo[2.2.1]hept-2-ene (M_2) and catalyst (Cat) in feed.
[b] Isolated yield based on total mass of M_1 and M_2.
[c] Measured by GPC analysis in THF.

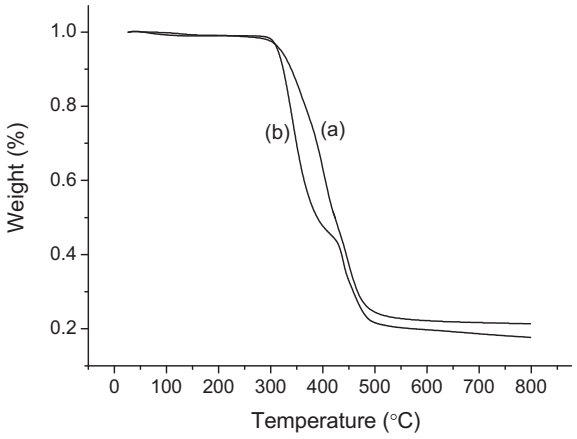

Fig. 2. The TGA curves for (a) copolymer **1** and (b) copolymer **2**.

3.2. Ring-opening metathesis copolymerization

The advantage of ROMP for the preparation of the copolymers is the ability to control the polymer molecular weight through the ratio of monomer to catalyst. To invest the tolerance of ruthenium initiator with cyano group, Ru-II is invited as an initiator because of its high functional group tolerance and well thermal stability [36]. ROM copolymerization of macromonomer and 5-cyano bicyclo [2.2.1]hept-2-ene is carried out under an inert atmosphere at 70 °C with macromonomer concentration of 0.01 mol L^{-1} in $CHCl_3$. The concentration of macromonomer is as low as 0.01 mol L^{-1} so that the chain could stretch for the catalyst approaching the double bond of norbornenyl group. In process of time an increase in solution viscosity is observed visually, which suggests the formation of the copolymer. After 12 or 24 h, the reaction is terminated with ethyl vinyl ether and the polymers are precipitated in methanol with about 50% yield. The synthetic route is illustrated in Scheme 1, and the characteristic features of the copolymers are listed in Table 2. It is seen that the relative high molecular weight copolymers are obtained which suggests the macromonomers have been converted to the copolymers. With the same ratio of monomer to catalyst, M_n of copolymer **2** is almost twice as much as that of copolymer **1** in proportion of the PCL side chain length. Comparing copolymers **2** and **3**, the yield and the M_n slightly increase with the excess of M_2. The M_w/M_n values for the copolymers are in the range from 1.55 to 1.78, which are rational for the copolymerization initiated by Ru-II as mentioned in the literature, where the polymerizations are usually not well controlled [34,37,38]. Nevertheless, there is still the improvement in polymerization performance of macromonomer at an appropriate condition as the steric crowding between macromonomers affects the rate of propagation k_p more than the rate of initiation k_i, contributing the lower ratio of k_p/k_i and the sterically hindrance of the side chain prevents the catalyst from reacting with the olefins along the backbone ("backbiting") [37,38]. Through the investigation in ROMP reactions of PCL-containing macromonomers [39], Kenwright et al. had revealed that the macromonomer with the lower ratio of $[M]_1/[Cat]$ and the shorter side chains would complete consumption of macromonomers. Thus, the really low ratio of 25:1 is employed in order to conduct the polymerization of the macromonomers favorably. However, the yield of the copolymer is no more than 54%. We presume that the low yield of the copolymers resulted from the low activity of the macromonomer with the bulky side chains and the monomer M_2 might poison the ruthenium catalyst to some extent [40].

Moreover, the representative ^1H NMR spectrum of the copolymer is presented in Fig. 1B. The chemical shift corresponding to olefinic signals on the norbornene ring (6.17 ppm) is instead by the proton signals at approximately 5.55–5.26 ppm after ring-opening, which indicates the subsequent polymerization is processed entirely. By comparing the peak integration areas (S) of methylene protons of CH_2 (H_p, 2 protons) at 2.06–1.93 ppm from norbornyl group of M_2 with those of olefinic protons of C*H*=C*H* (H_a, 4 protons) at 5.55–5.26 ppm on the PNBE backbone from the units of M_1 and M_2, it is possible to determine the molar ratio of M_2/M_1 from the integral ratio $x/y = (S_p/2H)$: $[(S_a - S_p)/2H] = S_p/(S_a - S_p) = 33$, which accords with the molar ratio calculated by elemental analysis from the formula: $M_2/M_1 = (w \times z\%/14)/\{[w - (w \times z\%)/14 \times 119]/M_{n,NBE\text{-}g\text{-}PCL}\} = 35$, where w is the weight of copolymer sample, z is the weight percent of nitrogen in M_2, 119 is the molar mass of M_2, and $M_{n,NBE\text{-}g\text{-}PCL}$ is the molar mass of M_1. The results display that M_2 has a higher tendency for incorporated into the copolymer than M_1, which attributes to the relatively low activity of macromonomer M_1 with bulky side chains.

3.3. Thermal stability and crystallinity

The thermal stability of the copolymers was evaluated by TGA in Fig. 2. A two-step degradation process is seen in the copolymer **2** (Fig. 2b) and the first-step is caused by the decomposition of crystal PCL side chains with the decomposition temperature in the range from 300 to 430 °C. A similar observation was reported in the literature [41], the polylactide-grafted NBE copolymers exhibited a two-step degradation process where the temperature range of the decomposition of thermally labile polylactide lay between 170 and 270 °C due to a signature of the random chain scission accompanied by transesterification reactions [42–45]. However, there is not an obvious two-step degradation of the copolymer **1** (Fig. 2a). We deduce that the copolymer **1** with better thermal stability and lower percentage of PCL content makes the two-step degradation invisible. As we knew, the thermal stability has largely depended on the length of PCL chain. The copolymer **2** with about 38 CL units is twice as much as the copolymer **1** with about 19 CL units for each PCL side chain, and the one with the longer PCL side chains is more inclined to thermal decomposition than that with the shorter. Moreover, by comparison of the temperature at which 10% weight loss of the copolymers in Table 3, we also see that the PNBE backbone with short PCL chains is more thermally stable.

Table 3
Thermal properties of copolymers.

Copolymer	$T_{d\ 5\%}$[a] (°C)	$T_{d\ 10\%}$[a] (°C)	T_g[b] (°C)	T_m[c] (°C)	T_c[c] (°C)	ΔH_f[c] (J g^{-1})	ΔH_c (J g^{-1})
1	320.0	340.2	nd[d]	nd	nd	nd	nd
2	314.0	323.9	−42.1	55.2	18.0	37.0	21.0

[a] Temperatures at 5% and 10% mass loss ($T_{d5\%}$ and $T_{d10\%}$) determined by TGA.
[b] Glass transition temperature measured by DMA.
[c] Melting temperature and crystallization temperature measured by DSC.
[d] Not detected.

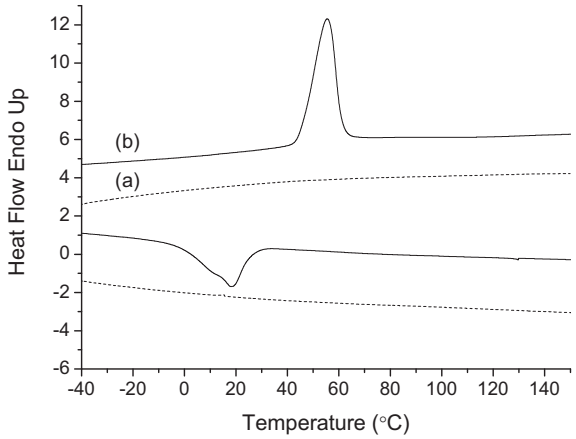

Fig. 3. DSC traces of second heating and cooling for copolymer **1** (a) and copolymer **2** (b).

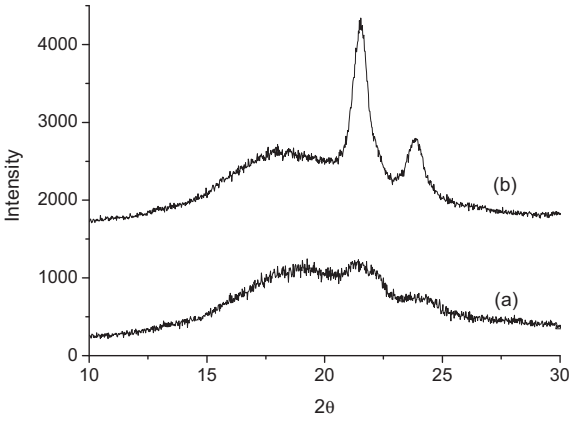

Fig. 4. X-ray diffraction pattern copolymer **1** (a) and copolymer **2** (b).

The DSC technique is invited to obtain the T_g, the melting temperature (T_m), the heat of crystallization (ΔH_c), and the heat of fusion (ΔH_f) that are summarized in Fig. 3 and Table 3. In order to erase any previous thermal history, two steps were performed. Firstly, the copolymers were heated to 240 °C and then cooled to −75 °C at a rate of 10 °C min^{-1}. Secondly, they were heated once more to 240 °C and cooled to −75 °C with the same heating and cooling rate. During the second heating and cooling cycle we obtained the values. From the curve, an endothermic peak is observed due to the melting of PCL crystalline phase in the copolymer **2**, and a T_m is measured in the peak maximum at 55.2 °C. The relevant melting enthalpy is 37.0 J g^{-1} which is lower than the perfect PCL crystal with a melting enthalpy of 140 J g^{-1} [46]. Correspondingly, an exothermic peak appears after the subsequent cooling crystallization and a T_c is detected in the peak maximum at 18.0 °C. However, no T_m is found in the copolymer **1**. According to the literature [47], the molecular weight of PCL side chains is the main factor to determine the crystallizability, for example, in the polyurethane-PCL copolymer when the molecular of PCL segment is less than 2000, the PCL phase isn't crystallized. Therefore, in the case of copolymer **1**, we deduce that the molecular weight about 2200 for each PCL side chain is too low to form the perfect crystalline phase for DSC detection. For comparison, the crystalline microstructures of the two copolymers are investigated by the X-ray diffraction pattern. As shown in Fig. 4b the copolymer **2** has two phases: one broad diffraction peak with a maximum around 18° 2θ indicates a typical amorphous pattern of PNBE [48,49] and two strong scattering peaks at $2\theta = 21°$(4.11 Å) and 24° (3.72 Å) indicates the crystallinity of PCL [7]. The copolymer **1** has the wide dispersion peaks instead of two strong scattering peaks, which indicates the crystalline region doesn't form by the shorter PCL side chains in accordance with the DSC analysis. On the whole, the copolymer **2** of two-phase structure is a potential polymer for use as a shape memory material. Thus DMA is introduced in the following for further characterization of the copolymer **2**.

3.4. Mechanical properties

Shape memory effects are the macroscopic reflection of internal molecular motions in the copolymers. When shape memory polymers are deformed by a periodic force, some of energy is stored and some energy is giving off in form of dissipated heat from molecular internal friction which is reflected in the change in loss tangent (tanδ) or loss modulus of the dynamic mechanical behavior against temperature. The DMA curve based on the molecular motion of polymers provides the information of transition temperatures.

As see in Fig. 5, the dynamic mechanical spectrum of the copolymer **2** depicts the dependence of storage modulus (E') and tanδ on temperature. The relaxation peaks obtained from each peak of loss modulus (E'') at −111.0 °C and −42.1 °C are related with sub-relaxation temperature (T_γ) and T_g in turn, which are higher than that obtained from the peaks of tanδ. The specimen is characterized by a solidlike storage modulus (about 4 GPa) for the temperature below −111 °C (T_γ) which is associated with the motion of $-CH_2-$ sequences in the PCL chain including the movement of oxygen atom [50]. During the calefactive process, the crystalline phase

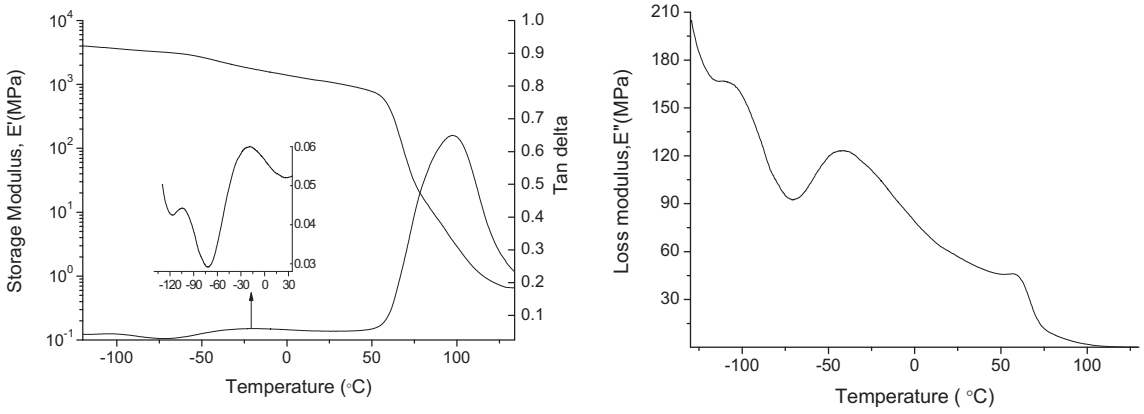

Fig. 5. DMA curves of the specimen made by copolymer **2**.

Table 4
Mechanical properties of copolymers.

Copolymer	Tensile modulus (MPa)	Tensile strength (MPa)	Yield strength (MPa)	Elongation at break (%)
1	20 ± 3.1	11.1 ± 2.5	3.4 ± 0.1	380 ± 18
2	30 ± 2.8	21.6 ± 3.4	4.3 ± 0.2	260 ± 10

works as underprop for keeping room temperature modulus. From the onset of T_g at −60 °C of PCL side chains, E′ begins to decrease gradually to a level of 1 GPa at room temperature. The rapidly fall of the E′ indicates that the copolymer exhibits the good shape fixity on cooling and the large shape recovery upon heating [7], whereas the elastic modulus ratio of the glass (E'_g) to rubber (E'_r) is often quoted to estimate the magnitude of the change in E'. Practically, the ratio of $E'_{trans-20°C}/E'_{trans+20°C}$ below and above the T_{trans} is usually measured. It is more visual to interpret the effect of the ratio on the shape memory ability combining with the curve of shape recovery versus temperature in Fig. 7. When the modulus is 915 MPa at 40 °C, the corresponding shape recovery is almost to nought while the modulus drops to 17.1 MPa at 80 °C, the corresponding shape recovery is more than 90%. The ratio calculated by $E'_{40°C}/E'_{80°C}$ = 915 MPa/17.1 MPa = 53.5 shows that the material has good shape memory effect. As the temperature approaching the T_m 55.2 °C, the E' curve decreases sharply which displays that the large-scale motion of the PCL side chains in the copolymer, and the thermally stable backbone prevents the chains from further disintegrating or disentanglement. We notice that the sharp increase in tanδ above T_{trans} might lead to the damping and irreversible deformation. Therefore, we estimate the flow temperature (T_{flow}) that defines as the temperature at which the E' falls below 1 MPa [51]. T_{flow} is an indicator of the upper temperature of the material cause the polymer would deform irreversibly above that. From the data of E', the T_{flow} is at 115 °C which is about 60 °C higher than T_{trans}, showing it is suitable as a shape memory material.

The stress–strain curves were obtained at room temperature and the results were listed in Table 4. As indicated in Fig. 6, the copolymer **1** behaves as an elastomer in the curve (a). A gradually steady increase of stress is observed without any stress plateau before the rupture. The curve (b) for copolymer **2** resembles the semi-crystalline polymers such as polyethylene and polypropylene. When the material reaches the ultimate tensile strength, yielding occurs, and the macroscopic change is observed subsequently. After the yield point, an obvious decrease in width of the sample

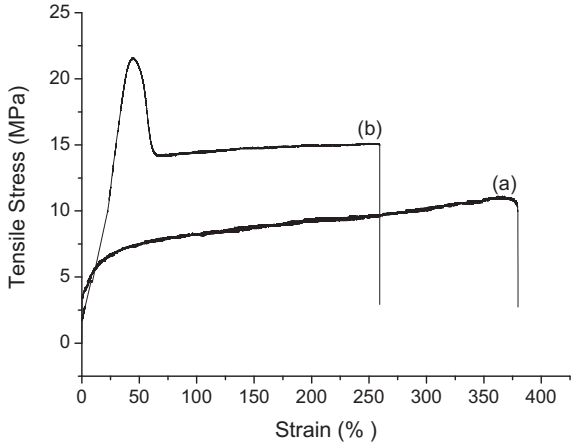

Fig. 6. Representative stress–strain curves for copolymer **1** (a) and copolymer **2** (b).

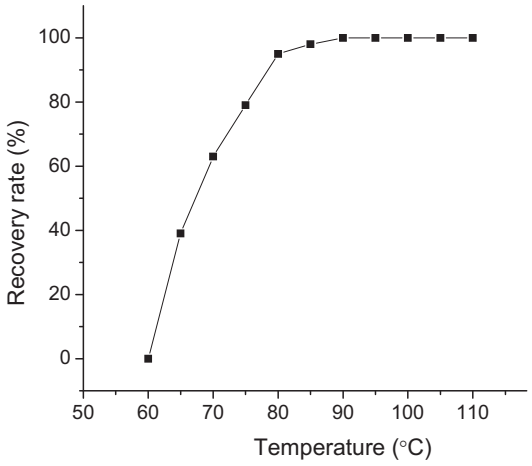

Fig. 7. Shape recovery rate against temperature for the copolymer **2**.

neck is seen till no further reduction in cross-section and the specimen breaks with the elongation of 260%. In analogy to semi-crystalline SMP [7], with the increase of the crystal PCL content, the modulus and yield strength increase while the elongation at break decreases.

3.5. Shape memory behavior

In our shape memory system, the melting transition of the crystalline PCL side chains acts as the T_{trans}, which also assumes the additional role of the physical cross-linking points before their melting. When the PCL crystallites melt above the T_m, the entanglement between the chains plays the role of physical cross-links which prevent the polymer from deforming irreversible. When the copolymer is heated above T_{trans} ($T_{trans} = T_m$), it can be deformed and the temporary shape is fixed by cooling the temperature below the T_c. Meanwhile the mechanical energy is stored. As a result of the restoration of the network chain conformational entropy, the copolymer is forced back to its original form. Shape recovery rate and shape recovery speed are two characters to evaluate the shape memory ability. Shape recovery rate is measured from the proportion of the maximum shape recovery angle to that of the original shape. Specifically, a dumbbell specimen was folded and cooled at room temperature. When the specimen was heated in a constant temperature for 30 min, the shape recovery angle (θ) was measured by the angle between the straight ends of the bent specimen [52]. The shape recovery rate (R) was calculated from the following equation:

$$R = (\theta/180) \times 100\% \ (0^\circ \le \theta \le 180^\circ)$$

Thus, we obtained a one-to-one relationship between the shape recovery rate and the temperature (Fig. 7) with the maximum error less than 5%. The heating temperature range was set from 60 to 110 °C at 5 °C interval. Clearly, the full recovery was observed at 90 °C which was about 35 °C above the T_{trans}. When the temperature was below the T_{trans}, the recovery rate was as low as 0°.

Shape recovery speed is also a vital character on which the application of SMP materials is depended. Fig. 8 shows the shape memory progress of a dumbbell type specimen. The specimen was heated to 90 °C, bent at 0° and cooled at room temperature to fix a temporary shape. When heated at a constant temperature 90 °C, the specimen was regained the permanent shape without any external stress within 5 min.

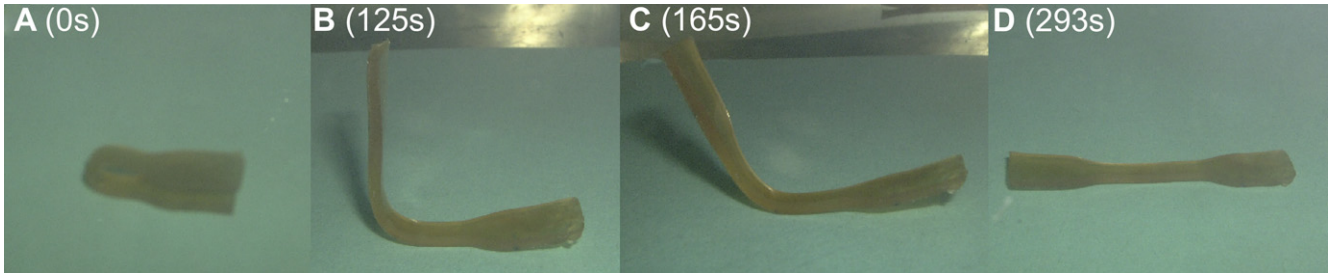

Fig. 8. The sequence of photos demonstrates the thermally induced shape memory effect of a dumbbell specimen. The specimen in its temporary folded shape (A) is heated in 90 °C. Within 293s the specimen recovers the permanent shape, a nearly planar strip (D) through the process (B) and (C) in which the angles are approximately 90° and 120° at 125s and 165s respectively.

4. Conclusions

A novel kind of the PNBE copolymer with the long PCL side chains and the cyano group was synthesized through ROMP under the mild reaction conditions for handling the mold and process challenges in the kind of PNBE shape memory materials. Two copolymers with different side chain lengths of PCL were obtained and the one with the longer chain length possessed the promising shape memory effect. From DMA curve, the fall of the storage modulus demonstrates that the copolymer has the good shape fixity and the large shape recovery, which indicates that it is suitable for use as a shape memory material. An actual trend in the polymer science is to design the materials with multi-functionality. In this work, the cyano group attached to the backbone provides the possibility of the further investigation in the additional magnetism function of the material through chelating iron oxide nanoparticles, and it is in progress.

Acknowledgements

The authors thank the National Natural Science Foundation of China (No. 50973030), Shanghai Municipality Commission for Special Project of Nanometer Science and Technology (Nos. 0852nm03200 and 0952nm05300), and International Corporation Project of Shanghai Municipality Commission (No. 10410710000) for the financial supports of this work.

References

[1] Lendlein A, Kelch S. Angew Chem Int Ed 2002;41:2034–57.
[2] Wei ZG, Sandström R, Miyazaki S. J Mater Sci 1998;33:3743–62.
[3] Wei ZG, Sandström R, Miyazaki S. J Mater Sci 1998;33:3763–83.
[4] Feninat FE, Laroche G, Fiset M, Mantovani D. Adv Eng Mater 2002;4:91–104.
[5] Schurch KE, Ashbee KHG. Nature 1977;266:706–7.
[6] Heuer AH, Ruhle M, Marshall DB. J Am Ceram Soc 1990;73:1084–93.
[7] Kim BK, Lee SY, Xu M. Polymer 1996;37:5781–93.
[8] Takahashi T, Hayashi N, Hayashv S. J Appl Polym Sci 1996;60:1061–9.
[9] Luo XF, Mather PT. Macromolecules 2009;42:7251–3.
[10] Knight PT, Lee KM, Chung T, Mather PT. Macromolecules 2009;42:6596–605.
[11] Zhang H, Wang HT, Zhong W, Du QG. Polymer 2009;50:1596–601.
[12] Domeier L, Nissen A, Goods S, Whinnery LR, McElhanon J. J Appl Polym Sci 2010;115:3217–29.
[13] Deka HK, Karak N. J Appl Polym Sci 2010;116:106–15.
[14] Inomata K, Nakagawa K, Fukuda C, Nakada Y, Sugimoto H, Nakanishi E. Polymer 2010;51:793–8.
[15] Voit W, Ware T, Dasari RR, Smith P. Adv Funct Mater 2010;20:162–71.
[16] Lee BS, Chun BC, Chung YC, Sul KI, Cho JW. Macromolecules 2001;34:6431–7.
[17] Lendlein A, Schmidt AM, Langer R. Proc Natl Acad Sci U S A 2001;98:842–7.
[18] Lendlein A, Langer R. Science 2002;296:1673–6.
[19] Yang JH, Chun BC, Chung YC, Cho JH. Polymer 2003;44:3251–8.
[20] Venkatraman SS, Tan LP, Joso JFD, Boey YCF, Wang X. Biomaterials 2006;27:1573–8.
[21] Yakacki CM, Shandas R, Lanning C, Rech B, Eckstein A, Gall K. Biomaterials 2007;28:2255–63.
[22] Ratna D, Karger-Kocsis J. J Mater Sci 2008;43:254–69.
[23] Dyana Merline J, Reghunadhan Nair CP, Gouri C, Sadhana R, Ninan KN. Eur Polym J 2007;43:3629–37.
[24] Chung YC, Shim YS, Chun BC. J Appl Polym Sci 2008;109:3533–9.
[25] Liu CD, Chun SB, Mather PT. Macromolecules 2002;35:9868–74.
[26] Liu CD, Chun SB, Mather PT. J Appl Med Polym 2002;6:47–52.
[27] Lendlein A, Neuenschwander P, Suter UW. Macromol Chem Phys 2000;201:1067–76.
[28] Bielawski CW, Grubbs RH. Prog Polym Sci 2007;32:1–29.
[29] Nishihara Y, Inoue Y, Nakayama Y, Shiono T, Takagi K. Macromolecules 2006;39:7458–60.
[30] Belfield KD, Zhang L. Chem Mater 2006;18:5929–36.
[31] Allcock HR, de Denus CR, Prange R, Laredo WR. Macromolecules 2001;34:2757–65.
[32] Zhang MJ, Flynn DL, Hanson PRJ. Org Chem 2007;72:3194–8.
[33] (a) Trollss M, Hedrick JL, Mecerreyes D, Dubois P, Jerome R, Ihre H, et al. Macromolecules 1997;30:8508–11;
(b) Bratton D, Brown M, Howdle SM. J Polym Sci Part A Polym Chem 2005;43:6573–85;
(c) Liu TQ, Simmons TL, Bohnsack DA, Mackay ME, Smith MR, Baker GL. Macromolecules 2007;40:6040–7;
(d) Hedrick JL, Carter KR, Richter R, Miller RD, Russell TP, Flores V. Chem Mater 1998;10:39–49.
[34] Czelusniak I, Khosravi E, Kenwright AM, Ansell CWG. Macromolecules 2007;40:1444–52.
[35] Zhu H, Deng GH, Chen YM. Polymer 2008;49:405–11.
[36] Scherman OA, Kim HM, Grubbs RH. Macromolecules 2002;35:5366–71.
[37] Jha S, Dutta S, Bowden NB. Macromolecules 2004;37:4365–74.
[38] Morandi G, Montembault V, Pascual S, Legoupy S, Fontaine L. Macromolecules 2006;39:2732–5.
[39] Quémener D, Chembot A, Héroguez V, Gnanou Y. Polymer 2005;46:1067–75.
[40] Trnka TM, Grubbs RH. Acc Chem Res 2001;34:18–29.
[41] Oh S, Lee JK, Theato P, Char K. Chem Mater 2008;20:6974–84.
[42] Zhao Y, Shuai X, Chen C, Xi F. Chem Mater 2003;15:2836–43.
[43] Boudouris BW, Frisbie CD, Hillmyer MA. Macromolecules 2008;41:67–75.
[44] Sivalingam G, Vijayalakshmi SP, Madras G. Ind Eng Chem Res 2004;43:7702–9.
[45] Sivalingam G, Karthik R, Madras GJ. Anal Appl Pyrolysis 2003;70:631–47.
[46] Crescenzi V, Manzini G, Calzolari G, Borri C. Eur Polym J 1972;8:449–63.
[47] Ping P, Wang WS, Chen XS, Jing XB. Biomacromolecules 2005;6:587–92.
[48] Vargas J, Martínez A, Santiago AA, Tlenkopatchev MA, Aguilar-Vega M. Polymer 2007;48:6546–53.
[49] Haselwander TFA, Heitz W, Krügel SA, Wendorff JH. Macromol Chem Phys 1996;197:3435–53.
[50] Reding FP, Fanden JA, Whitman RD. J Polym Sci 1962;57:483–98.
[51] Rabani G, Luftmann H, Kraft A. Polymer 2006;47:4251–60.
[52] Leng JS, Wu XL, Liu YJ. J Appl Polym Sci 2009;114:2455–60.